

ANL/NDM--78

DE83 005665

ANL/NDM-78

FAST-NEUTRON TOTAL AND ELASTIC-SCATTERING
CROSS SECTIONS OF ELEMENTAL INDIUM*

by

A. B. Smith, P. T. Guenther, and J. F. Whalen
Applied Physics Division

November, 1982

DISCLAIMER

This document was developed as an account of work sponsored by an agency of the United States Government. Neither the United States Government nor any agency thereof, makes any warranty, express or implied, or assumes any liability or responsibility for the accuracy, completeness, or usefulness of any information, apparatus, product, or process disclosed, or represents that its use would not infringe privately owned rights. Reference herein to any specific commercial product, process, or service by trade name, trademark, manufacturer, or otherwise does not necessarily constitute or imply its endorsement, recommendation, or favoring by the United States Government or any agency thereof. The views and opinions of authors expressed herein do not necessarily state or reflect those of the United States Government or any agency thereof.

*This work supported by the U.S. Department of Energy

Argonne National Laboratory
9700 South Cass Avenue
Argonne, Illinois 60439
USA

DISTRIBUTION OF THIS DOCUMENT IS UNLIMITED

NUCLEAR DATA AND MEASUREMENTS SERIES

The Nuclear Data and Measurements Series presents results of studies in the field of microscopic nuclear data. The primary objective is the dissemination of information in the comprehensive form required for nuclear technology applications. This Series is devoted to: a) measured microscopic nuclear parameters, b) experimental techniques and facilities employed in measurements, c) the analysis, correlation and interpretation of nuclear data, and d) the evaluation of nuclear data. Contributions to this Series are reviewed to assure technical competence and, unless otherwise stated, the contents can be formally referenced. This Series does not supplant formal journal publication but it does provide the more extensive information required for technological applications (e.g., tabulated numerical data) in a timely manner.

INFORMATION ABOUT OTHER ISSUES IN THE ANL/NDM SERIES:

A list of titles and authors for reports ANL/NDM-1 through ANL/NDM-50 can be obtained by referring to any report of this series numbered ANL/NDM-51 through ANL/NDM-77. Requests for a complete list of titles or for copies of previous reports should be directed to:

Section Secretary
Applied Nuclear Physics Section
Applied Physics Division
Building 316
Argonne National Laboratory
9700 South Cass Avenue
Argonne, Illinois 60439
USA

- ANL/NDM-51 Measured and Evaluated Neutron Cross Sections of Elemental Bismuth by A. Smith, P. Guenther, D. Smith and J. Whalen, April 1980.
- ANL/NDM-52 Neutron Total and Scattering Cross Sections of ^6Li in the Few MeV Region by P. Guenther, A. Smith and J. Whalen, February 1980.
- ANL/NDM-53 Neutron Source Investigations in Support of the Cross Section Program at the Argonne Fast-Neutron Generator by James W. Meadows and Donald L. Smith, May 1980.
- ANL/NDM-54 The Nonelastic-Scattering Cross Sections of Elemental Nickel by A. B. Smith, P. T. Guenther and J. F. Whalen, June 1980.
- ANL/NDM-55 Thermal Neutron Calibration of a Tritium Extraction Facility using the $^6\text{Li}(\text{n},\text{t})^4\text{He}/^{197}\text{Au}(\text{n},\gamma)^{198}\text{Au}$ Cross Section Ratio for Standardization by M. M. Bretscher and D. L. Smith, August 1980.
- ANL/NDM-56 Fast-Neutron Interactions with ^{182}W , ^{184}W and ^{186}W by P. T. Guenther, A. B. Smith and J. F. Whalen, December 1980.
- ANL/NDM-57 The Total, Elastic- and Inelastic-Scattering Fast-Neutron Cross Sections of Natural Chromium, Peter T. Guenther, Alan B. Smith and James F. Whalen, January 1981.
- ANL/NDM-58 Review of Measurement Techniques for the Neutron Capture Process by W. P. Poenitz, August 1981.
- ANL/NDM-59 Review of the Importance of the Neutron Capture Process in Fission Reactors, Wolfgang P. Poenitz, July 1981.
- ANL/NDM-60 Neutron Capture Activation Cross Sections of ^{94}Zr , ^{96}Zr , $^{98,100}\text{Mo}$, and $^{110,114,116}\text{Cd}$ at Thermal and 30 keV Energy, John M. Wyrick and Wolfgang P. Poenitz, (to be published).

ANL/NDM-61 Fast-neutron Total and Scattering Cross Sections of ^{58}Ni by Carl Budtz-Jørgensen, Peter T. Guenther, Alan B. Smith and James F. Whalen, September 1981.

ANL/NDM-62 Covariance Matrices and Applications to the Field of Nuclear Data, by Donald L. Smith, November 1981.

ANL/NDM-63 On Neutron Inelastic-Scattering Cross Sections of ^{232}Th , ^{233}U , ^{235}U , ^{238}U , ^{239}U , and ^{239}Pu and ^{240}Pu by Alan B. Smith and Peter T. Guenther, January 1982.

ANL/NDM-64 The Fission Fragment Angular Distributions and Total Kinetic Energies for $^{235}\text{U}(\text{n},\text{f})$ from 0.18 to 8.83 MeV by James W. Meadows, and Carl Budtz-Jørgensen, January 1982.

ANL/NDM-65 Note on the Elastic Scattering of Several MeV Neutrons from Elemental Calcium by Alan B. Smith and Peter T. Guenther, March 1982.

ANL/NDM-66 Fast-neutron Scattering Cross Sections of Elemental Silver by Alan B. Smith and Peter T. Guenther, May 1982.

ANL/NDM-67 Non-evaluation Applications for Covariance Matrices by Donald L. Smith, July 1982.

ANL/NDM-68 Fast-neutron Total and Scattering Cross Sections of ^{103}Rh by Alan B. Smith, Peter T. Guenther and James F. Whalen, July 1982.

ANL/NDM-69 Fast-neutron Scattering Cross Sections of Elemental Zirconium by Alan B. Smith and Peter T. Guenther (to be published).

ANL/NDM-70 Fast-neutron Total and Scattering Cross Sections of Niobium by Alan B. Smith, Peter T. Guenther and James F. Whalen, July 1982.

ANL/NDM-71 Fast-neutron Total and Scattering Cross Sections of Elemental Palladium by Alan B. Smith, Peter T. Guenther and James F. Whalen, June 1982.

ANL/NDM-72 Fast-neutron Scattering from Elemental Cadmium by Alan B. Smith and P. T. Guenther (to be published).

ANL/NDM-73 Fast-Neutron Elastic-Scattering Cross Sections of Elemental Tin by C. Budtz-Jørgensen, P. Guenther and A. Smith, July 1982.

ANL/NDM-74 Evaluation of the ^{238}U Neutron Total Cross Section by W. Poenitz, A. B. Smith and R. Howerton (to be published).

ANL/NDM-75 Neutron Total and Scattering Cross Sections of Elemental Antimony by A. B. Smith, P. T. Guenther, and James F. Whalen, September 1981.

ANL/NDM-76 Scattering of Fast-Neutrons from Elemental Molybdenum by A. B. Smith and P. T. Guenther (to be published).

ANL/NDM-77 A Least-Squares Method for Deriving Reaction Differential Cross Section Information from Measurements Performed in Diverse Neutron Fields by Donald L. Smith, November 1982.

Table of Contents

ABSTRACT	vi
I. INTRODUCTION	1
II. BRIEF OUTLINE OF EXPERIMENTAL METHODS.	1
III. EXPERIMENTAL RESULTS	2
IV. INTERPRETATION AND DISCUSSION.	4
V. COMPARISONS WITH ENDF/B-V	6
VI. CONCLUDING COMMENTS.	6
ACKNOWLEDGEMENTS	9
REFERENCES	10

FAST-NEUTRON TOTAL AND ELASTIC-SCATTERING
CROSS SECTIONS OF ELEMENTAL INDIUM*

by

A. B. Smith, P. T. Guenther and J. F. Whalen

Applied Physics Division
Argonne National Laboratory

ABSTRACT

Broad-resolution neutron total cross sections of elemental indium were measured from 0.8 to 4.5 MeV. Differential-elastic-scattering cross sections were measured from \approx 1.5 to 3.8 MeV at intervals of \approx 50 to 200 keV and at scattering angles in the range 20 to 160 degrees. The experimental results are interpreted in terms of the optical-statistical model and are compared with respective values given in ENDF/B-V.

*This work supported by the U.S. Department of Energy.

I. INTRODUCTION

The present work is a part of a comprehensive study of the interaction of fast neutrons with fission-product nuclides in the mass region $A=89$ to 123 . The objectives were the explicit provision of relevant experimental data and the development of a "regional" optical-statistical model (OM) suitable for the prediction of neutron interactions with similar, but unmeasurable, fission-product nuclides.¹ Other aspects of this program are described in references 2 to 10.

Elemental indium is very nearly monoisotopic ($\approx 96\%$ ^{115}In).¹¹ Its fission-product yield is relatively small (e.g., 0.02% for thermal neutron induced fission of ^{233}U). ^{115}In is one $g_{9/2}$ proton short of the closed shell at $N=50$. The isomeric level at 336 keV ($1/2^-$, $t_{1/2}=4.5$ hours) is often employed in dosimetry applications. Twenty five levels have been reported over the excitation-energy range 0.5 to 2.0 MeV,^{11,12} or an average excited-level spacing of ≈ 60 keV. This profusion of levels makes the direct observation of inelastically-scattered neutrons due to the excitation of resolved discrete levels exceedingly tedious and a more promising experimental approach is the ($n;n'$, gamma) technique with its superior resolution¹², even considering gamma-decay uncertainties. Therefore, the present neutron measurements were confined to determinations of neutron total and elastic-scattering cross sections using sufficiently broad resolutions to reasonably assure a determination of the energy-average cross-section behavior consistent with the underlying concepts of the OM. Subsequent portions of this report deal with; i) a brief outline of the experimental method, ii) the experimental results, iii) an interpretation of the measured values in terms of the OM, and iv) some comparisons of the experimental results with the respective evaluated quantities given in ENDF/B-V.¹³

II. BRIEF OUTLINE OF EXPERIMENTAL METHODS

The measurement sample was a cylinder 2 cm in diameter and 2 cm long, machined from chemically pure indium metal. The sample density was determined from precise weight and dimension measurements and there was no evidence of sample non-uniformity. All the measurements employed the $^7\text{Li}(p;n)^7\text{Be}$ reaction as a neutron source¹⁴, pulsed on for durations of ≈ 1 nsec at a repetition rate of 2 MHz. The mean neutron energy was determined to within ± 10 keV by control of the incident-proton beam and it was verified by the observation of well known neutron-total-cross-section resonances.¹⁵ The incident-neutron energy spread was determined by the thickness of the lithium-target film.

The neutron total cross sections were deduced from the observed transmissions of essentially monoenergetic neutrons through the measurement sample in the conventional manner.¹⁶ The measurements were made using the Argonne total-cross-section apparatus described in Ref. 17. A massive shield and collimator system was arranged about the neutron source so as to provide a 1 cm diameter neutron beam at a zero-degree source-reaction angle. The transmission sample was placed upon a rotating wheel about 1 m from the source and the wheel rotated in a stepping motion so as to interchange measurement samples and voids approximately 50 times a minute. This sample motion averaged possible beam-intensity fluctuations and made independent monitoring of source

intensity unnecessary. In addition to the indium sample, the measurements always included a carbon reference sample and, usually, several samples with well known resonances. The neutron detector was a proton-recoil scintillator placed approximately 4 m from the source on the beam axis. Conventional time-of-flight techniques were used to control the background and to separate the primary neutron group of the source reaction from the second, and minority, neutron group. In-scattering corrections were estimated and found to be negligible. A random pulser, multiplexed in the measurement system, insured proper correction for dead-time effects. Details of the neutron total-cross-section apparatus and measurement techniques are given in Refs. 17 and 18.

The neutron elastic-scattering cross sections were measured using the Argonne ten-angle time-of-flight system.¹⁹ The scattering sample was placed approximately 13 cm from the source at a zero-degree source reaction angle. Ten flight paths were defined by massive collimators, distributed between scattering angles of 20 to 160 degrees. Relative scattering angles were known to ± 0.1 degrees and the absolute scale to ± 0.6 degrees. The neutron detectors were proton-recoil scintillators placed approximately 5.4 m from the scattering sample. The scattered-neutron velocity resolution was ample for the separation of elastically-scattered neutrons from all known inelastically-scattered neutrons. The relative responses of the detectors were determined by the observation of neutrons emitted at the spontaneous fission of ^{252}Cf .²⁰ These relative detector responses were then normalized to the measured neutron total cross sections of carbon in the manner described in Ref. 21. This detector-calibration method implies scattering cross sections essentially independent of any reference standard. The elastic-scattering cross sections were deduced from the observed velocity spectra using the data-reduction techniques described in Ref. 22. These included corrections for multiple-event, beam-attenuation and angular-resolution effects using a combination of analytical and Monte-Carlo calculational procedures.

III. EXPERIMENTAL RESULTS*

A. Neutron Total Cross Sections

The neutron total cross sections were measured from ≈ 0.8 to 4.5 MeV in steps of ≈ 50 keV with incident-neutron resolutions of 50 to 70 keV. The measurement range was traversed several times with consistent results. The measured values were combined and averaged over 50 keV incident-neutron energy intervals to obtain the final results shown in Fig. 1. The statistical uncertainties of the averaged values were $\leq 1\%$. Systematic uncertainties were believed to be $\lesssim 1\%$. In particular, self-shielding effects were estimated at the lower energies using the methods of Ref. 17 and found to be approximately equivalent to or less than the above statistical uncertainties. The present experimental results are in very good agreement with the neutron total cross sections recently measured by Poenitz and Whalen in an entirely independent set of experiments¹³, as illustrated in Fig. 1.

*Numerical results of this work have been transmitted to the National Nuclear Data Center, Brookhaven National Laboratory.

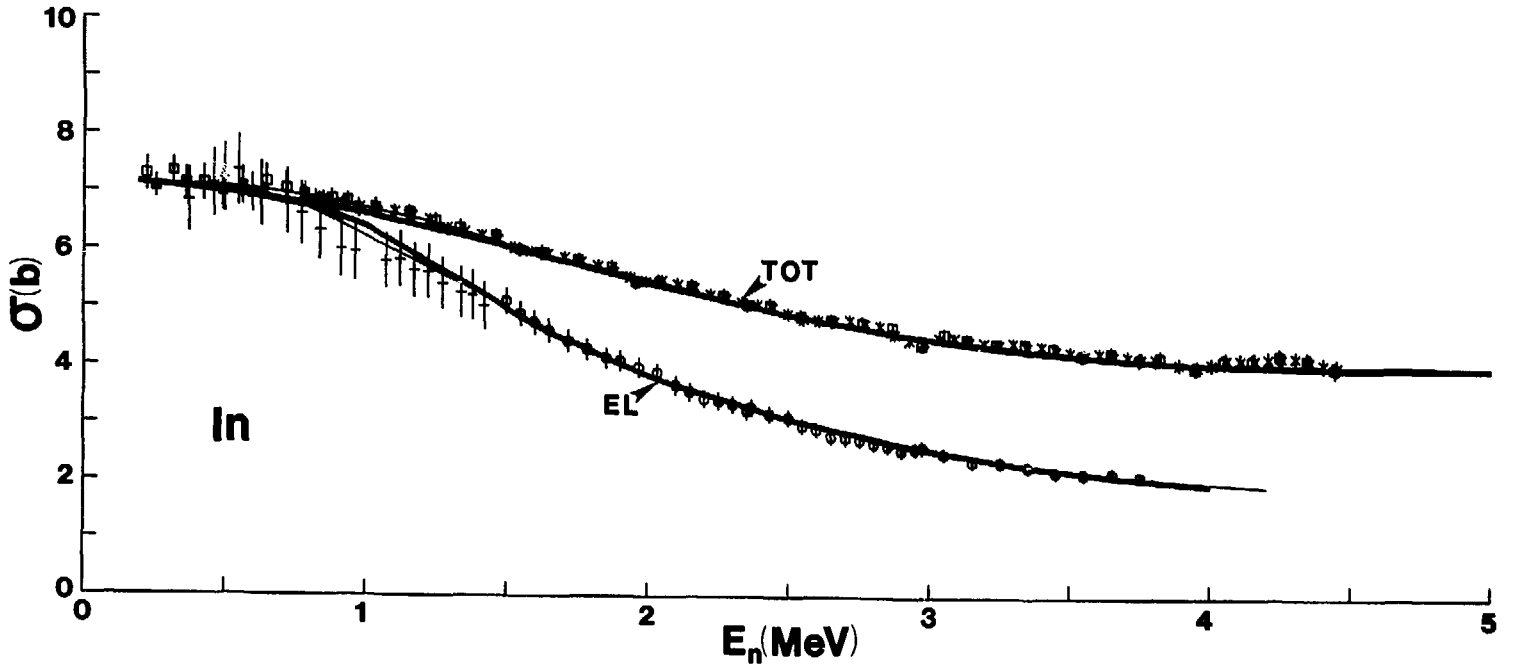


Fig. 1. Neutron Total and Elastic-Scattering Cross Sections of Elemental Indium. The present experimental results are indicated by \times (total cross sections) and \circ (angle-integrated elastic-scattering cross sections). The neutron total cross sections of Ref. 23 are noted by \square symbols and the lower-energy elastic-scattering results of Ref. 24 by $+$. Light curves are "eyeguides" constructed through the measured values and heavy curves indicate the results of calculations as described in the text.

B. Neutron Elastic-Scattering Cross Sections

The neutron elastic-scattering cross sections were measured from 1.5 to 3.75 MeV in steps of $\lesssim 50$ keV below 3.0 MeV and in 100 keV steps at higher energies. Below 3.0 MeV the measurements were made at ten scattering angles distributed between 20 and 160 degrees. At higher energies twenty scattering angles were used. The statistical uncertainties of the measured differential values were $\lesssim 1\%$, except near the minima of the higher-energy distributions. The detector calibrations were believed known to within $\approx 3\%$. Correction procedures introduced an additional uncertainty of $\lesssim 1\%$. Thus, the overall differential-cross-section uncertainties were $\lesssim 5\%$, again excepting the extreme minima of the higher-energy distributions. The measured differential-elastic-scattering cross sections and their respective uncertainties are illustrated in Fig. 2. These experimental results were least-square fitted with 6th-order Legendre-Polynomial series to obtain the angle-integrated elastic-scattering cross sections shown in Fig. 1. The angle-integrated cross-section uncertainties were estimated to be $\approx 5\%$. The Legendre fitting procedure provided a good description of the differential experimental values, as illustrated in Fig. 2. Neither the differential elastic-scattering cross sections, nor the angle-integrated values, nor the measured neutron total cross sections, displayed any significant energy-dependent fluctuations. The present elastic-scattering results are in good agreement with the lower-energy results reported from this Group a number of years ago.²⁴ The differential values of the two data sets reasonably extrapolate to one another near 1.5 MeV, as illustrated in Fig. 2, and there is a similar consistency between angle-integrated elastic-scattering values, as illustrated in Fig. 1.

IV. INTERPRETATION AND DISCUSSION

The interpretation was based upon the measured differential elastic-scattering cross sections, assuming the concept of a spherical optical-statistical model (OM).²⁵ The model parameters were determined by simultaneously chi-square fitting the differential elastic-scattering cross sections of Fig. 2; concurrently varying real and imaginary strengths, radii and diffusenesses. The data base was not of sufficient energy scope to clearly indicate the potential energy dependence. Therefore a real energy dependence of the form $V = V_0 - 0.3 \times E(\text{MeV})$ was assumed, in accord with proposed "global" models.²⁶ The imaginary strength was assumed to be energy independent. An additional assumption was a spin-orbit potential of the Thomas form with a 6 MeV strength and the geometry of the real potential. The experimental data base is in a transitional region. At the lower measured energies, compound-elastic-scattering (CE) cross sections were appreciable and at the higher energies the elastic-scattering cross sections were very largely due to shape-elastic-scattering (SE) processes. The CE contributions were calculated using the Hauser-Feshbach formula,²⁷ as modified by Moldauer.²⁸ The calculations explicitly treated the excitation of nineteen discrete levels up to excitation energies of ≈ 1.6 MeV, assuming the energies, spins and parities of Ref. 11. Higher-energy excitations were represented by the statistical formalism and parameters of Gilbert and Cameron.²⁹ Radiative capture cross sections were relatively very small and thus were ignored in the fitting procedures. All calculations were carried out using the computer code ABAREX³⁰.

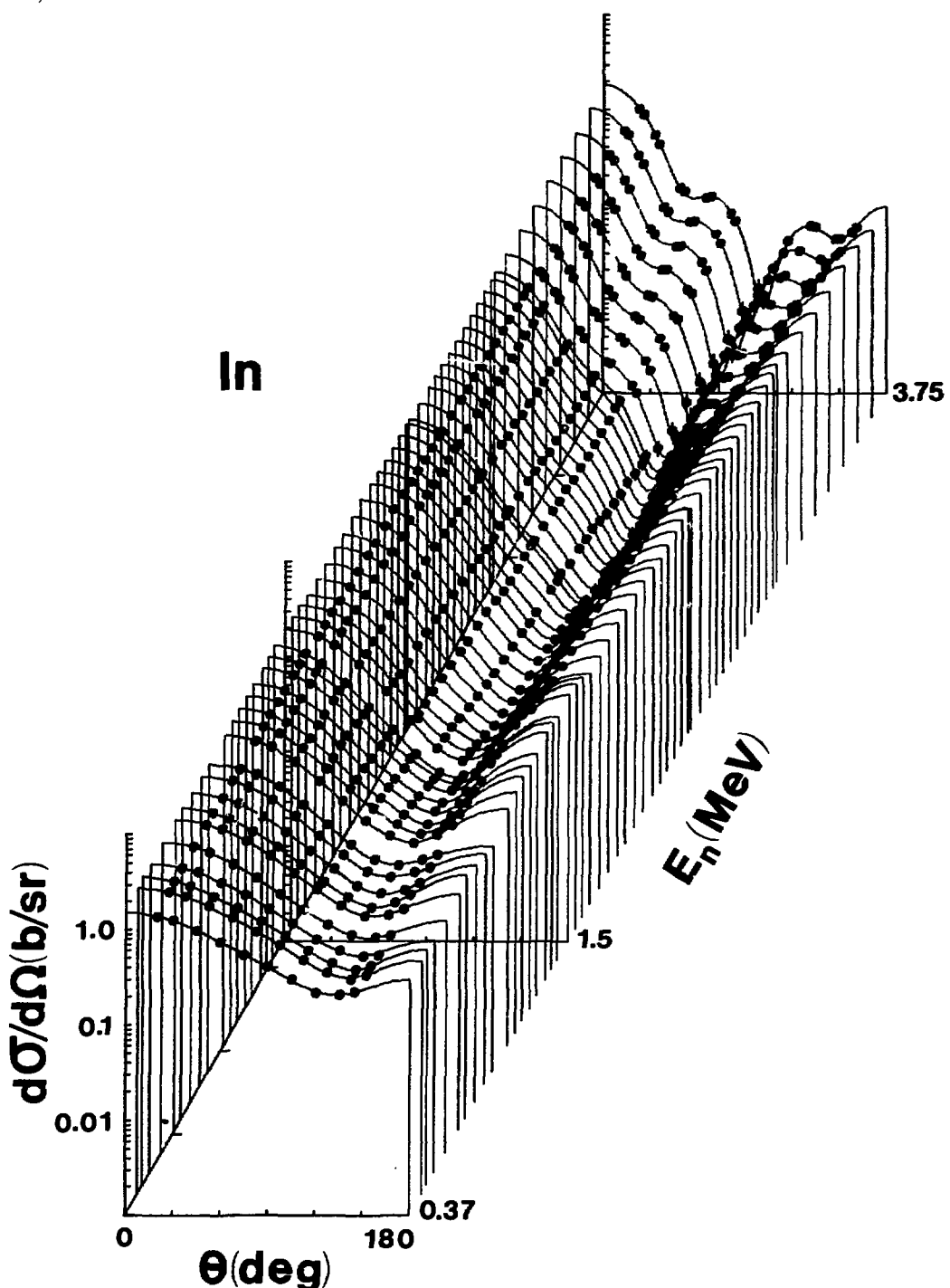


Fig. 2. Differential Elastic-Scattering Cross Sections of Elemental Indium. The present experimental results are indicated by data symbols above 1.5 MeV, those of Ref. 24 by symbols below 1.5 MeV. Curves indicate the results of fitting Legendre-Polynomial series to the measured values as described in the text.

The target spin is large ($9/2^+$) and a number of differential elastic-scattering distributions were involved in the fitting procedures. Thus the calculations were somewhat tedious but they steadily converged to the parameters given in Table 1. These parameters are similar to those previously found to be suitable in this mass-energy region.²⁻¹⁰ The imaginary radius is larger than that of the real potential, as is commonly observed in potentials based upon low-energy strength functions.³¹ The parameters of Table 1 provide a very good description of the observed differential elastic-scattering cross sections, as illustrated in Fig. 3. The calculated and measured values are generally consistent to within the experimental uncertainties. There are minor differences between measured and calculated results at the extreme minima of the distributions near ≈ 2.0 MeV where the calculations are particularly sensitive to the CE contribution. In this region the CE contribution is largely determined by the low-excitation energies of the statistical level representation. There may be considerable deviations from the general statistical parameters of Ref. 29 in this low-energy region. This minor shortcoming can be alleviated by modification of the statistical-level parameterization but such parameter-adjustment procedures were not pursued. The parameters of Table 1 also provide a very good description of the measured neutron total and angle-integrated elastic-scattering cross sections, as illustrated in Fig. 1. More than 90% of the measured values agree with the calculated results to within the experimental uncertainties alone.

V. COMPARISONS WITH ENDF/B-V

ENDF/B-V¹³ contains ^{113}In (MAT-9473) and ^{115}In (MAT-9477) evaluated files. These two isotopic files were combined to obtain an elemental file for comparison with the present experimental results. Comparisons of measured and evaluated neutron total and elastic-scattering cross sections are illustrated in Fig. 4 and some comparative numerical values are given in Table 2. The evaluated neutron total cross sections are generally lower than the measured values; increasingly so as the energy decreases. The differences are several times the experimental uncertainties. Above ≈ 2.0 MeV, the evaluated elastic-scattering cross sections are considerably larger than the measured values by amounts that are 3 to 5 times the experimental uncertainties. These differences are reflected in the nonelastic cross section where that implied by the evaluation is 30% to 50% smaller than that indicated by the measurements over much of the experimental energy range. The nonelastic discrepancies are large and will be reflected in the inelastic-scattering cross sections above ≈ 2.0 MeV.

VI. CONCLUDING COMMENTS

The present measurements give improved definition to the neutron total and elastic-scattering cross sections of elemental indium in the few-MeV region. Parameters of an optical-statistical model were deduced from the measured elastic-scattering cross sections. This model provides a very good description of the observed cross sections and is a suitable vehicle for extrapolation to both lower and higher energies. The model parameters are similar to those generally found applicable to this mass-energy region and are used for the development of a general "regional" model to be described elsewhere.¹

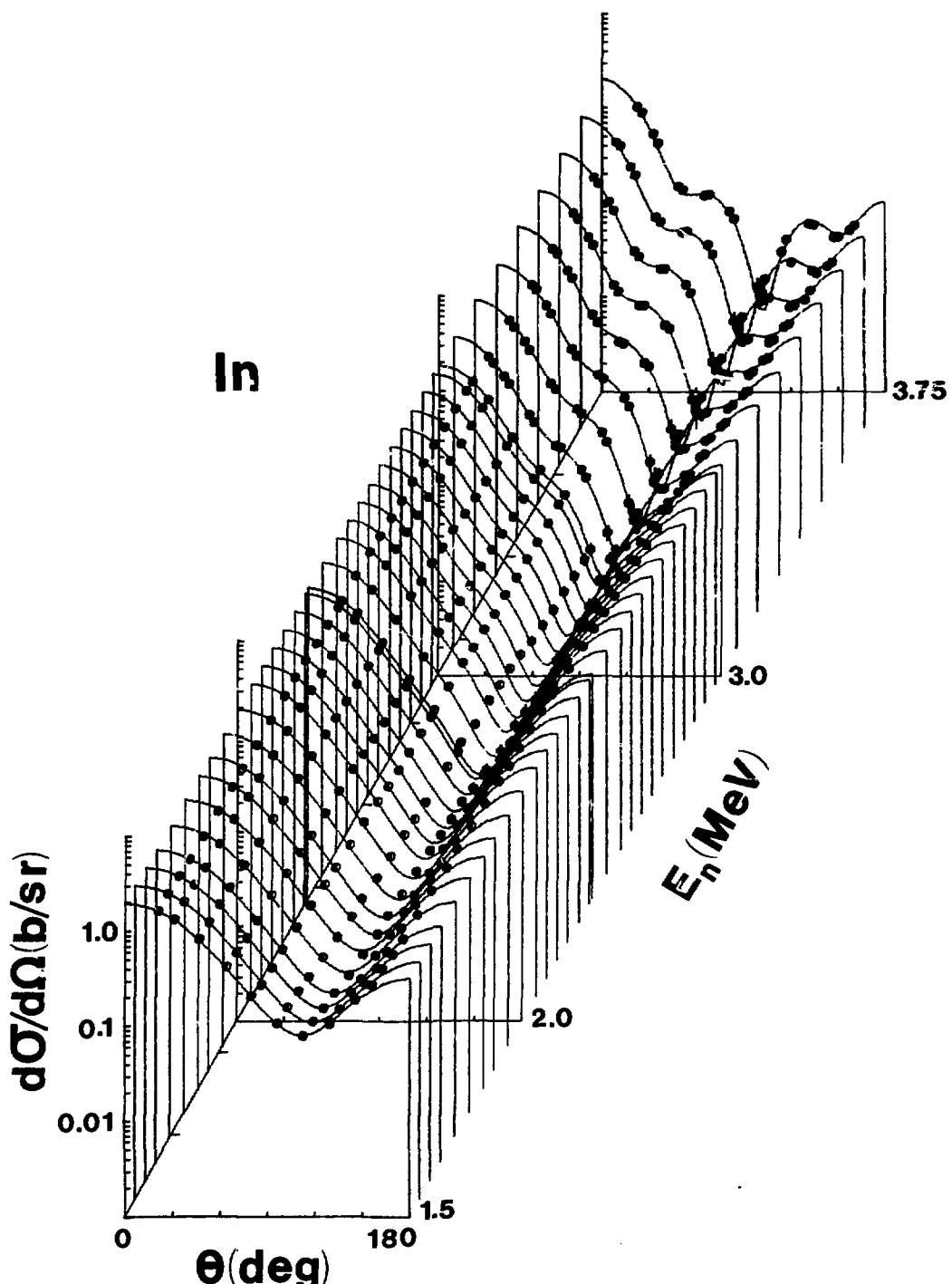


Fig. 3. Comparisons of Measured and Calculated Differential-Elastic-Scattering Cross Sections of Elemental Indium. The present experimental values are indicated by data symbols and the results of calculation by curves.

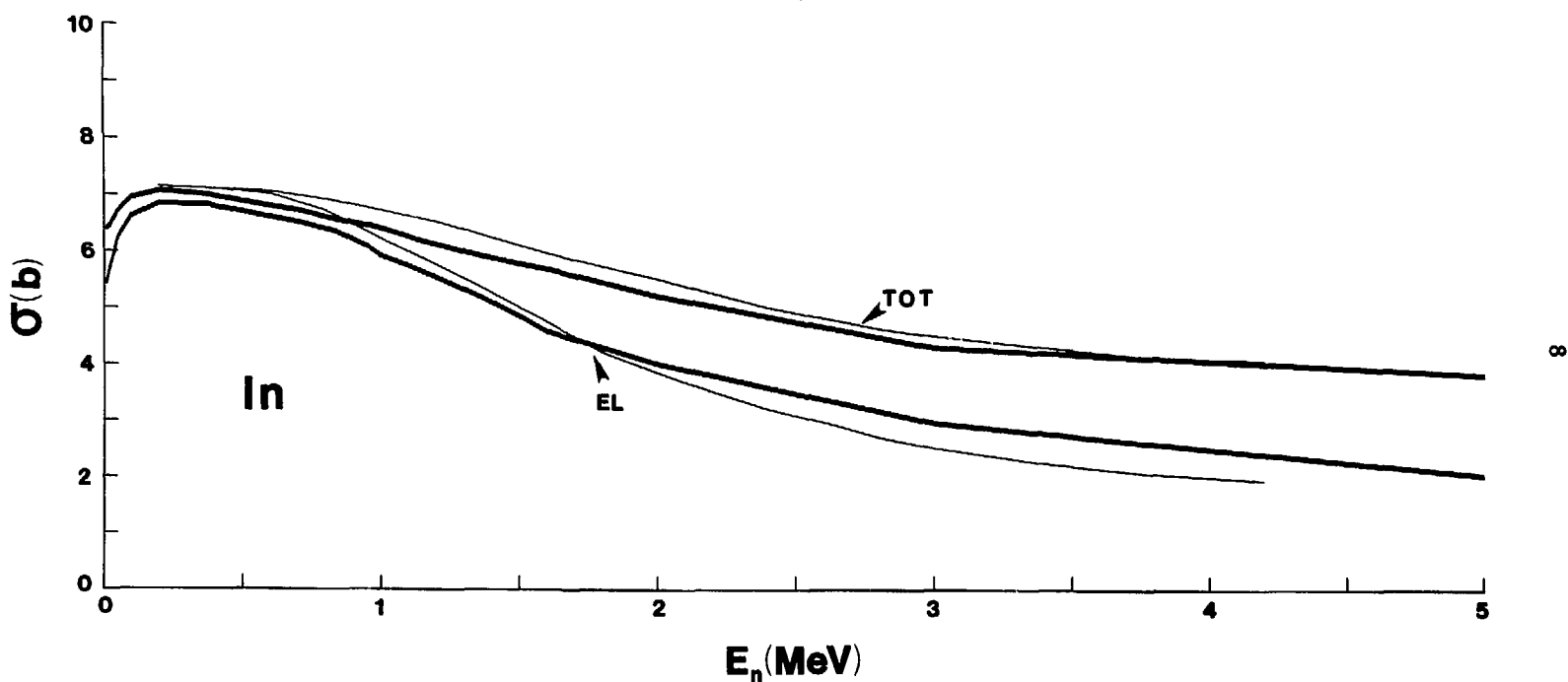


Fig. 4. Comparisons of Measured and Evaluated Neutron Total and Elastic-Scattering Cross Sections of Elemental Indium. The ENDF/B-V¹³ values are indicated by heavy curves and the present experimental results by "eyeguides" (light curves).

The measured neutron total cross sections are consistently larger than those given by ENDF/B-V and the measured elastic-scattering cross sections are smaller than the evaluated quantities above ≈ 2.0 MeV. A consequence of this are large differences between nonelastic cross sections as deduced from the measurements and the evaluation and these differences will be reflected in the inelastic-scattering cross section.

ACKNOWLEDGEMENTS

The authors are indebted to: Dr. P. A. Moldauer for helpful suggestions, Dr. W. P. Poenitz for the provisions of pre-publication data, and to Dr. E. Pennington for assistance in handling the ENDF/B-V file.

REFERENCES

1. A. B. Smith, to be published.
2. A. Smith and P. Guenther, Argonne National Laboratory Report, ANL/NDM-66 (1982).
3. A. Smith, P. Guenther and J. Whalen, Argonne National Laboratory Report, ANL/NDM-68(1982).
4. A. Smith, P. Guenther and J. Whalen, Argonne National Laboratory Report, ANL/NDM-69 (1982).
5. A. Smith, P. Guenther and J. Whalen, Argonne National Laboratory Report, ANL/NDM-70 (1982).
6. A. Smith, P. Guenther and J. Whalen, Argonne National Laboratory Report, ANL/NDM-71 (1982).
7. A. Smith and P. Guenther, Argonne National Laboratory Report, ANL/NDM-72 (1982).
8. C. Budtz-Jorgensen, P. Guenther and A. Smith, Argonne National Laboratory Report, ANL/NDM-73 (1982).
9. A. B. Smith, P. T. Guenther and J. F. Whalen, Argonne National Laboratory Report, ANL/NDM-75 (1982).
10. A. B. Smith and P. T. Guenther, Argonne National Laboratory Report, ANL/NDM-76 (1982).
11. Table of Isotopes, 7th Edition, C. M. Lederer and V. S. Shirley Eds., John Wiley and Sons, Inc., New York (1978).
12. I. Van Heerden, private communication.
13. Evaluated Nuclear Data File-B, Version V, Brookhaven National Laboratory Report, ENDF-201 (1979), compiled by R. Kinsey.
14. J. W. Meadows and D. L. Smith, Argonne National Laboratory Report, ANL-7938 (1972).
15. INDC/NEANDC Nuclear Standards File, 1980 Version, A. B. Smith Ed., INDC-36/LN, IAEA Press, Vienna (1981).
16. D. Miller, Fast-Neutron Physics, Vol.-II, J. Marion and J. Fowler Eds., Interscience Pub., New York (1963).
17. W. Poenitz, A. Smith and J. Whalen, Nucl. Sci. and Eng., 78 333 (1981).
18. P. T. Guenther and A. B. Smith, Phys Rev., in press.

REFERENCES (Contd.)

19. A. B. Smith, P. Guenther, R. Larsen, C. Nelson, P. Walker and J. Whalen, Nucl. Instr. and Methods, 50 277 (1967).
20. A. B. Smith, P. Guenther and R. Sjoblom, Nucl. Instr. and Methods, 140 397 (1977).
21. A. Smith and P. Guenther, Argonne National Laboratory Report, ANL/NDM-63 (1982).
22. P. T. Guenther, Elastic and Inelastic Neutron Scattering of Fast-Neutrons from the Even Isotopes of Tungsten, University of Illinois Thesis (1977).
23. W. P. Poenitz and J. F. Whalen, private communication.
24. W. G. Vonach and A. B. Smith, Nucl. Phys., 78 389 (1966).
25. P. Hodgson, Nuclear Reactions and Nuclear Structure, Clarendon Press, Oxford (1971).
26. J. Rapaport, V. Kulkarni and R. Finley, Nucl. Phys., A330 15 (1979).
27. W. Hauser and H. Feshbach, Phys. Rev., 87 366 (1952).
28. P. A. Moldauer, Phys. Rev., C11 426 (1978).
29. A. Gilbert and A. Cameron, Can. Jour. Phys., 43 1446 (1965).
30. ABAREX, a Spherical Optical-Model Code, P. Moldauer, private communication (1982).
31. P. A. Moldauer, Nucl. Phys., 47 65 (1963).

Table 1. Optical-Model Potential Parameters^a

Real Potential ^b		
Strength	$V_0 = 47.285$	MeV
Radius ^c	$R_V = 1.267$	F
Diffuseness	$a_V = 0.644$	F
J/A_V ^d	$= 446.0 \text{ MeV} \times F^3$	
Imaginary Potential ^e		
Strength	$W_0 = 8.494$	MeV
Radius	$R_W = 1.317$	F
Diffuseness	$a_W = 0.406$	F
J/A_W	$= 62.64 \text{ MeV} \times F^3$	

^aAssume spin-orbit term of Thomas form with 6 MeV strength and the geometry of the real potential.

^bSaxon form, assume energy dependence of $V = V_0 - 0.3 E(\text{MeV})$.

^cAll radii expressed as $R = R_1 \times A^{1/3}$.

^dIntegral per nucleon.

^eSaxon-derivative form.

Table 2. Comparisons with ENDF/B-V¹³

E_n (MeV)	ENDF-EXP		
	σ_t	σ_{e1}	σ_{none1}
1.0	-4.6	-	-
1.5	-6.1	-5.6	-19.6
2.0	-5.8	+3.3	-37.5
2.5	-3.1	+10.9	-44.1
3.0	-4.6	+14.2	-48.1
3.5	-1.7	+18.8	-36.6
4.0	-0.5	+20.0	-33.8